

*Synergistic effect between PPy:PSS copolymers and biomass-derived activated carbons: A simple strategy for designing sustainable high-performance Li-S batteries*

Fernando Luna-Lama,<sup>a</sup> Alvaro Caballero<sup>a</sup> Julián Morales<sup>a,\*</sup>

<sup>a</sup>Dpto. Química Inorgánica e Ingeniería Química, Instituto de Química Fina y Nanoquímica, Universidad de Córdoba, Córdoba, 14071, Spain

\*Corresponding Author: [iq1mopaj@uco.es](mailto:iq1mopaj@uco.es); Tel.: +34-957-218620

**Supplementary Information**

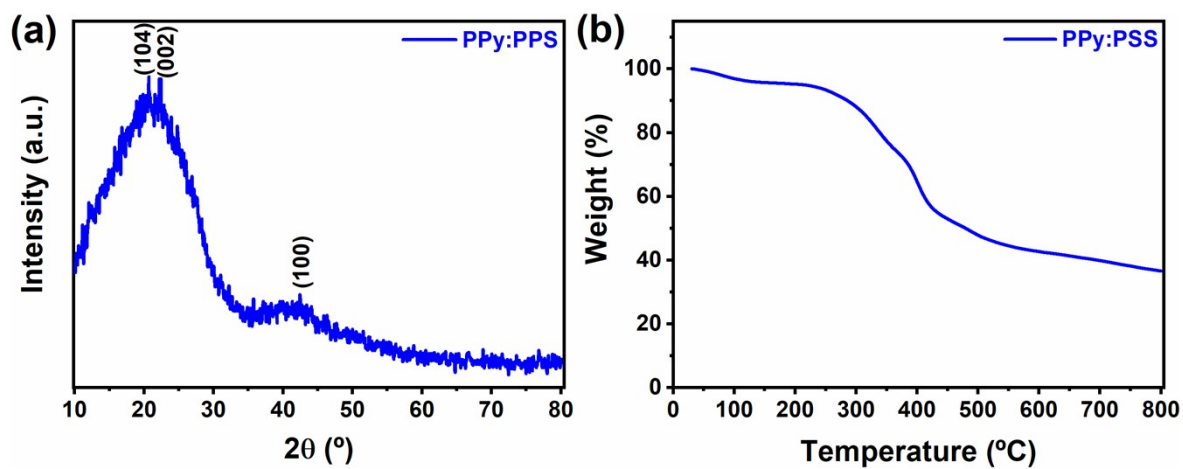


**Figure S1.** (a) XRD pattern. (b) TGA curve recorded in N<sub>2</sub> of PPy:PSS copolymer.

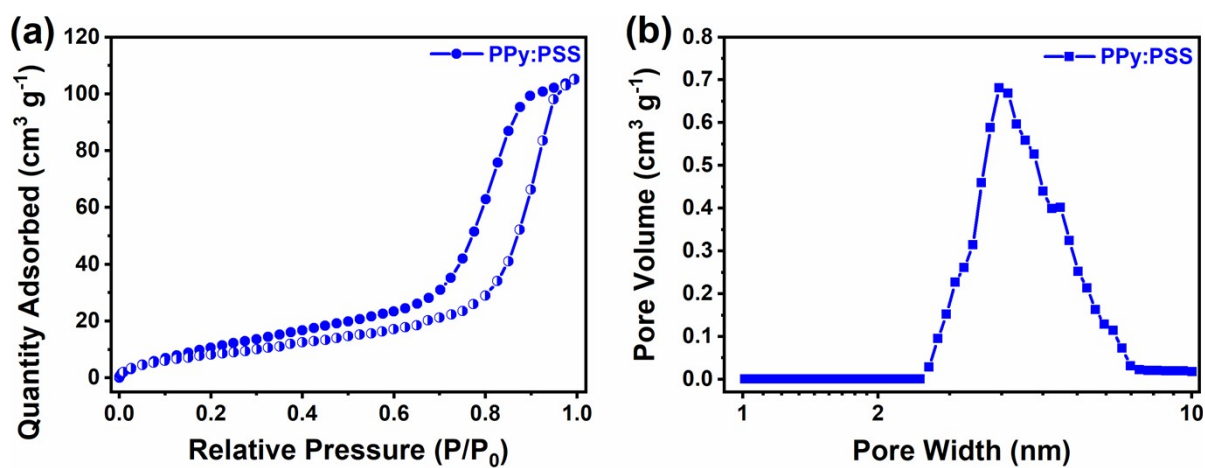


**Figure S2.** (a)  $N_2$  adsorption/desorption isotherm. (b) Pore size distribution of PPy:PSS copolymer.

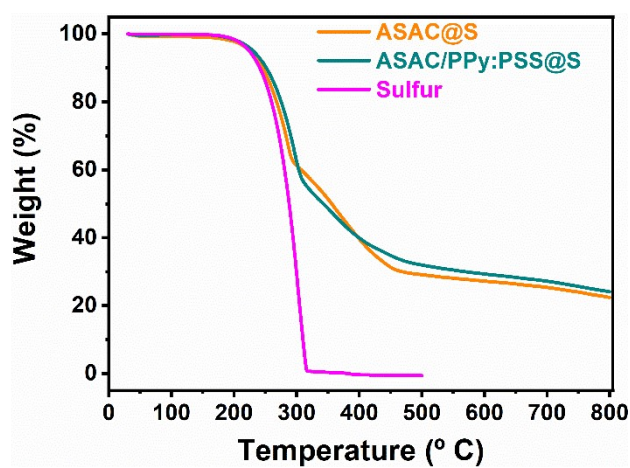


**Figure S3.** TGA curves recorded under  $N_2$  of pure S and ASAC@S and ASAC/PPy:PSS@S composites.

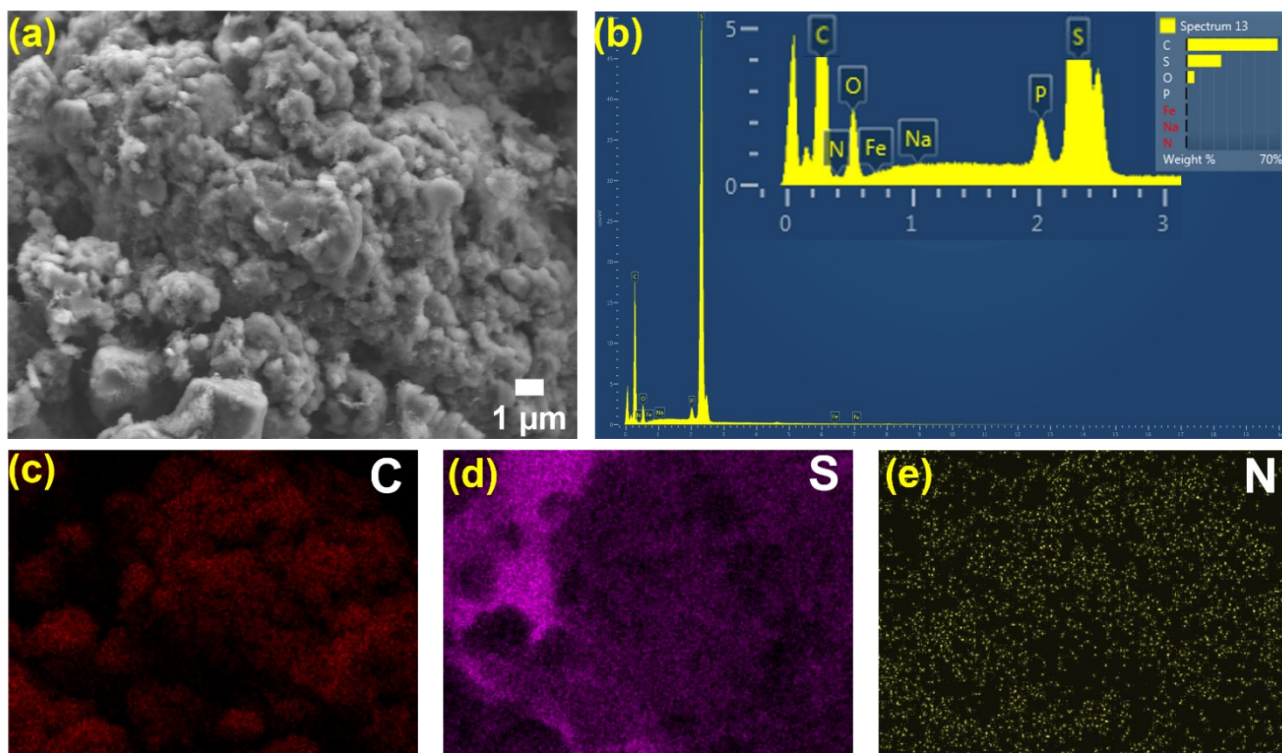


**Figure S4.** (a) SEM image. (b) EDX spectrum. In the insert, the plot scale is enlarged.

. (c) C, (d) S, and (e) N elemental mappings of ASAC/PPy:PSS@S composite.

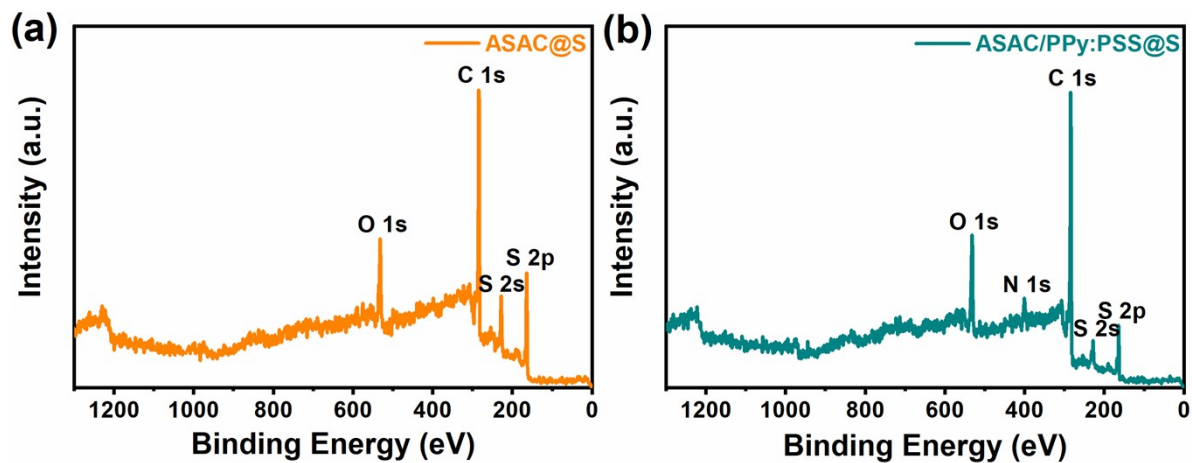


**Figure S5.** XPS survey spectra of (a) ASAC@S and (b) ASAC/PPy:PSS@S composites.

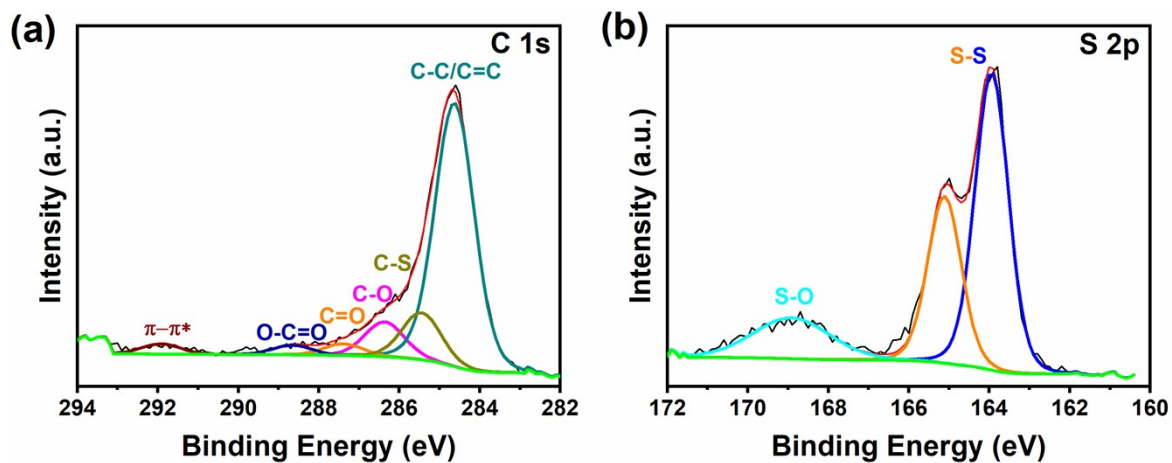


**Figure S6.** XPS spectra of (a) C 1s, (b) S 2p for the ASAC@S composite.

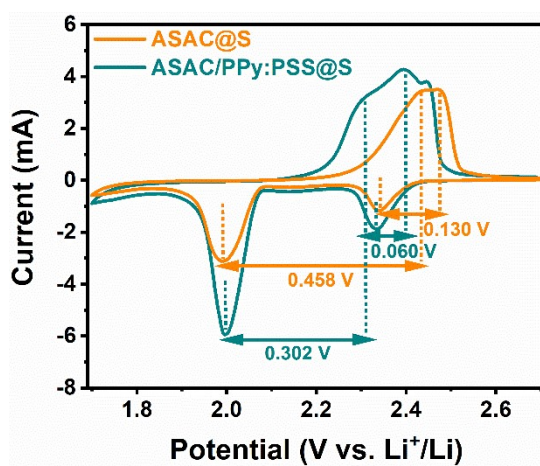


**Figure S7.** Polarization values ( $\Delta E$ ) between the cathode and anode peaks of the composite electrodes.

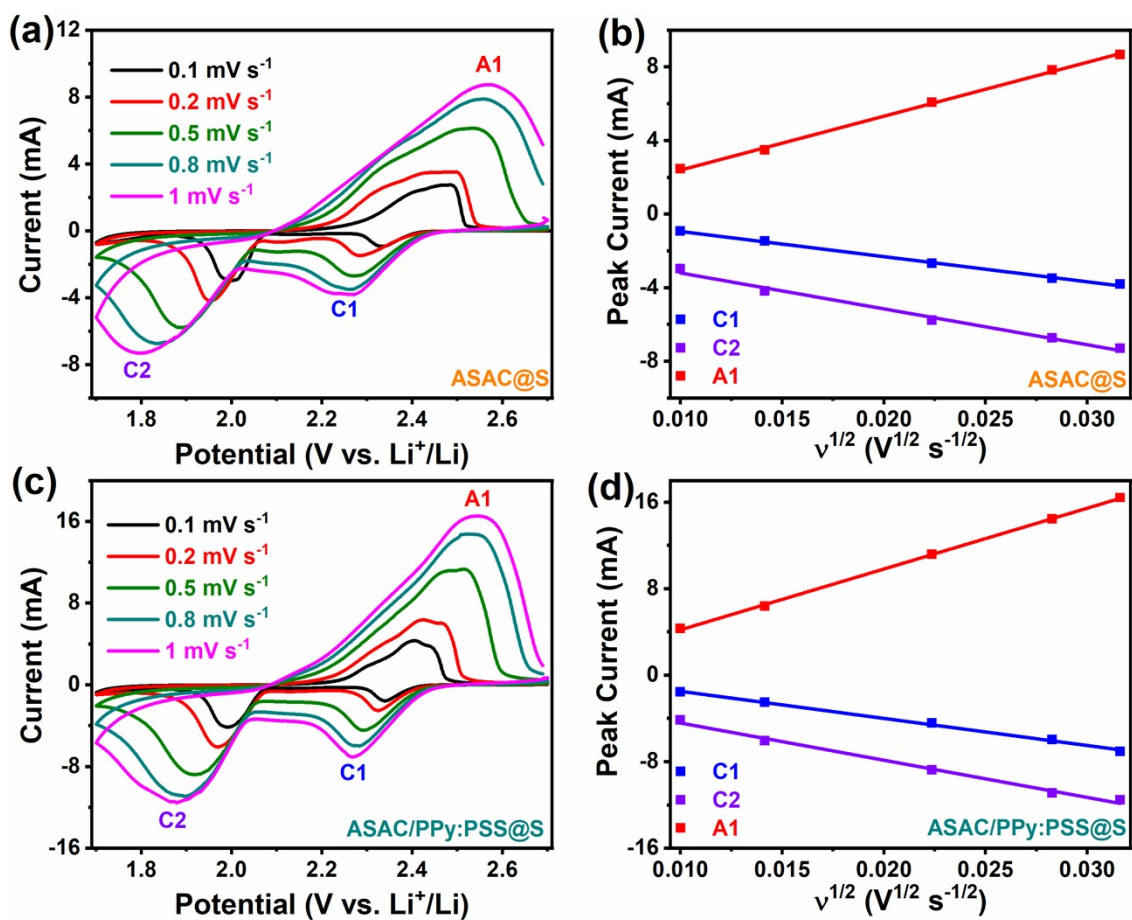


**Figure S8.** (a), (c) CV curves of the composite electrodes at various scan rates from 0.1 to 1 mV s<sup>-1</sup>. (b), (d) The corresponding fitted plots of the Randles–Sevcik equation applied to the cathode and anode peaks.

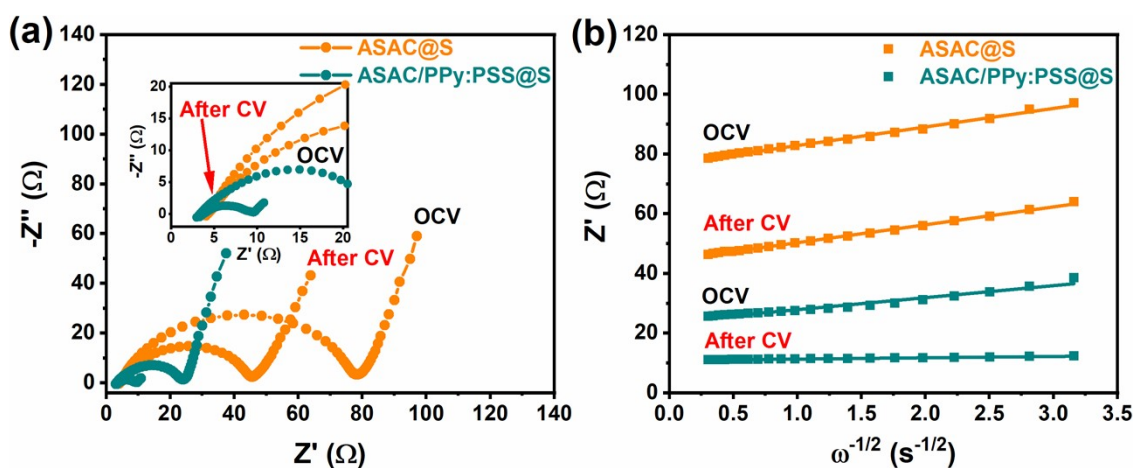


**Figure S9.** (a) EIS spectra of the composite electrodes recorded in a frequency range from 0.1 Hz to 500 kHz at OCV and after CV recorded at a potential scanning rate of  $0.1 \text{ mV s}^{-1}$ . In the insert, the plot scale is enlarged. (b) The corresponding fitted plot of the real part  $Z'$  of the impedance as a function of the inverse square root of angular frequency range from  $0.316$  to  $3.16 \text{ s}^{-1/2}$  (frequency range from 10 to 0.1 Hz) for the electrode composites.

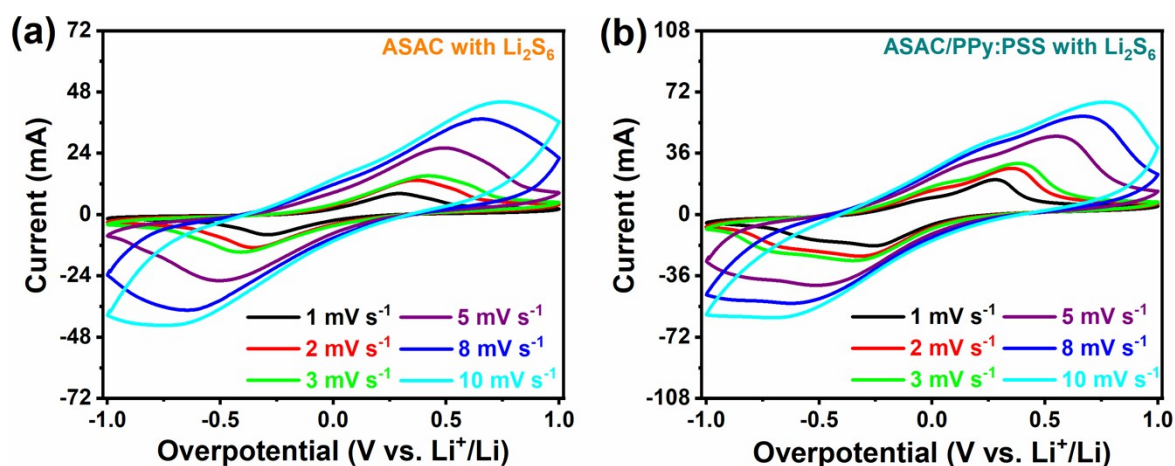


**Figure S10.** Polarization curves of symmetric cells with  $\text{Li}_2\text{S}_6$  of: (a) ASAC. (b) ASAC/PPy:PSS free-sulfur matrix electrodes. The curves were recorded at scan rate from 1 to  $10 \text{ mV s}^{-1}$ .

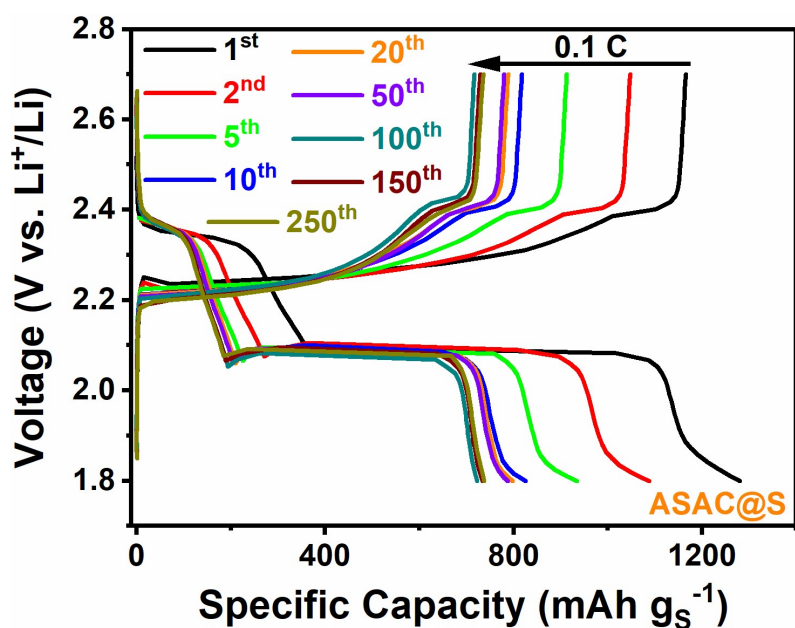


**Figure S11.** Discharge-charge profiles of the ASAC@S electrode at 0.1C. Electrode sulfur loading:  
 $2.0 \text{ mg cm}^{-2}$ .

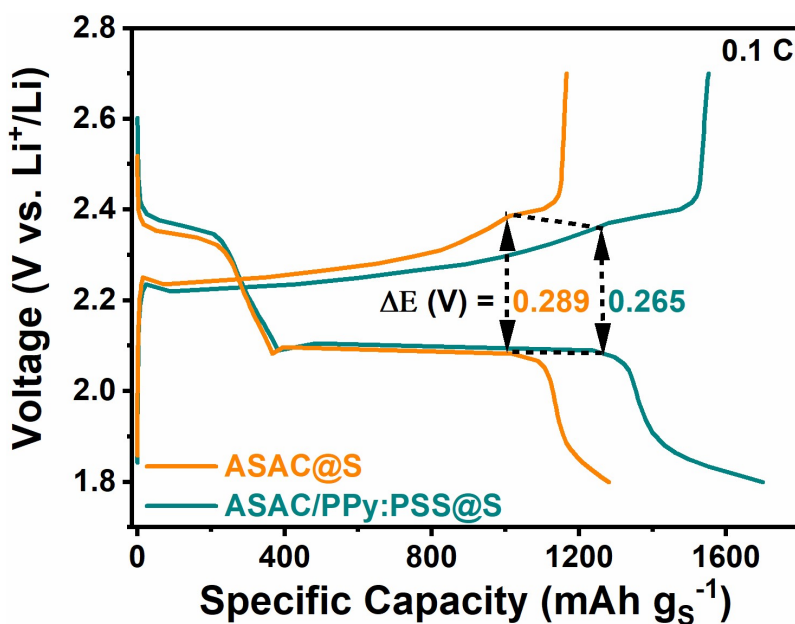


**Figure S12.** Polarization values ( $\Delta E$ ) between the discharge and charge curves of the electrodes recorded at 0.1C. Electrode sulfur loading:  $2.0 \text{ mg cm}^{-2}$ .

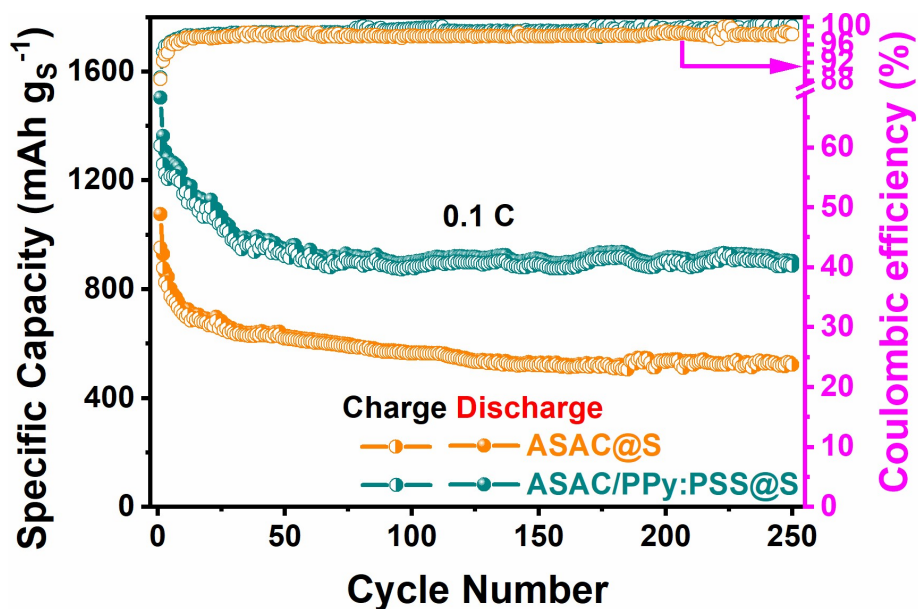


**Figure S13.** Variation of the discharge capacity as a function of the cycle number at 0.1 C with a sulfur loading of  $6 \text{ mg cm}^{-2}$  for the composite electrodes. Electrode sulfur loading:  $6.0 \text{ mg cm}^{-2}$ .

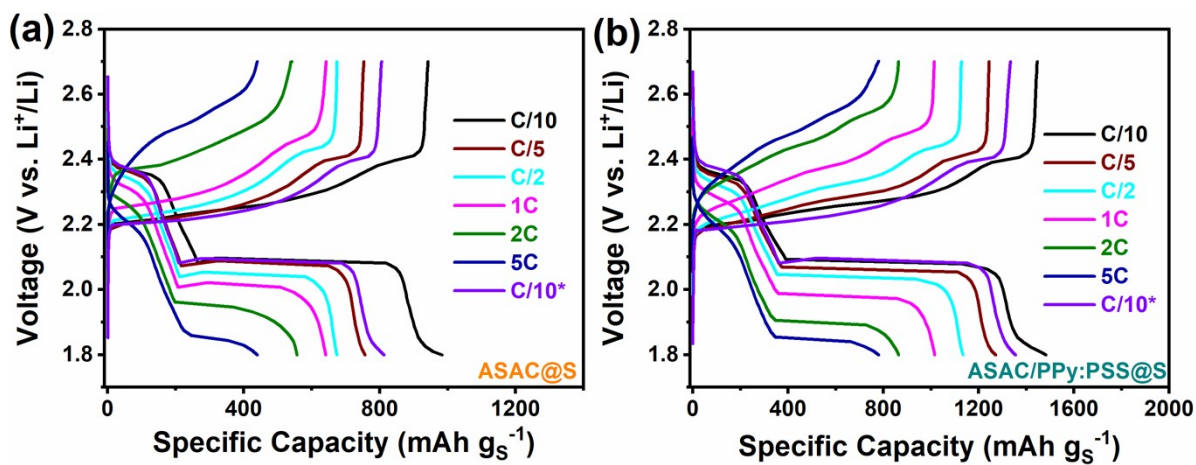


**Figure S14.** Discharge-charge profiles recorded at different current rates. (a) ASAC@S and (b) ASAC/PPy:PSS@S electrodes. Electrode sulfur loading:  $2.0 \text{ mg cm}^{-2}$ .



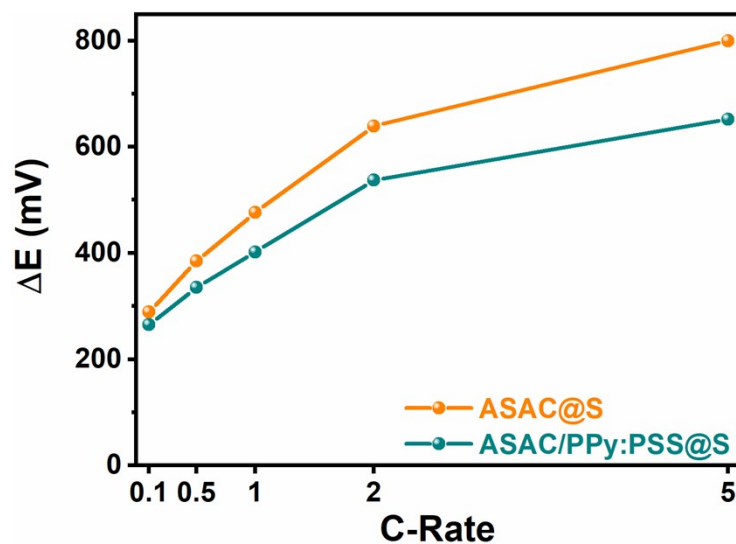


**Figure S15.** Variation of the polarization ( $\Delta E$ ) between the discharge and charge curves as a function of the current rates (values obtained from rate capability curves). Electrode sulfur loading:  $2.0 \text{ mg cm}^{-2}$ .

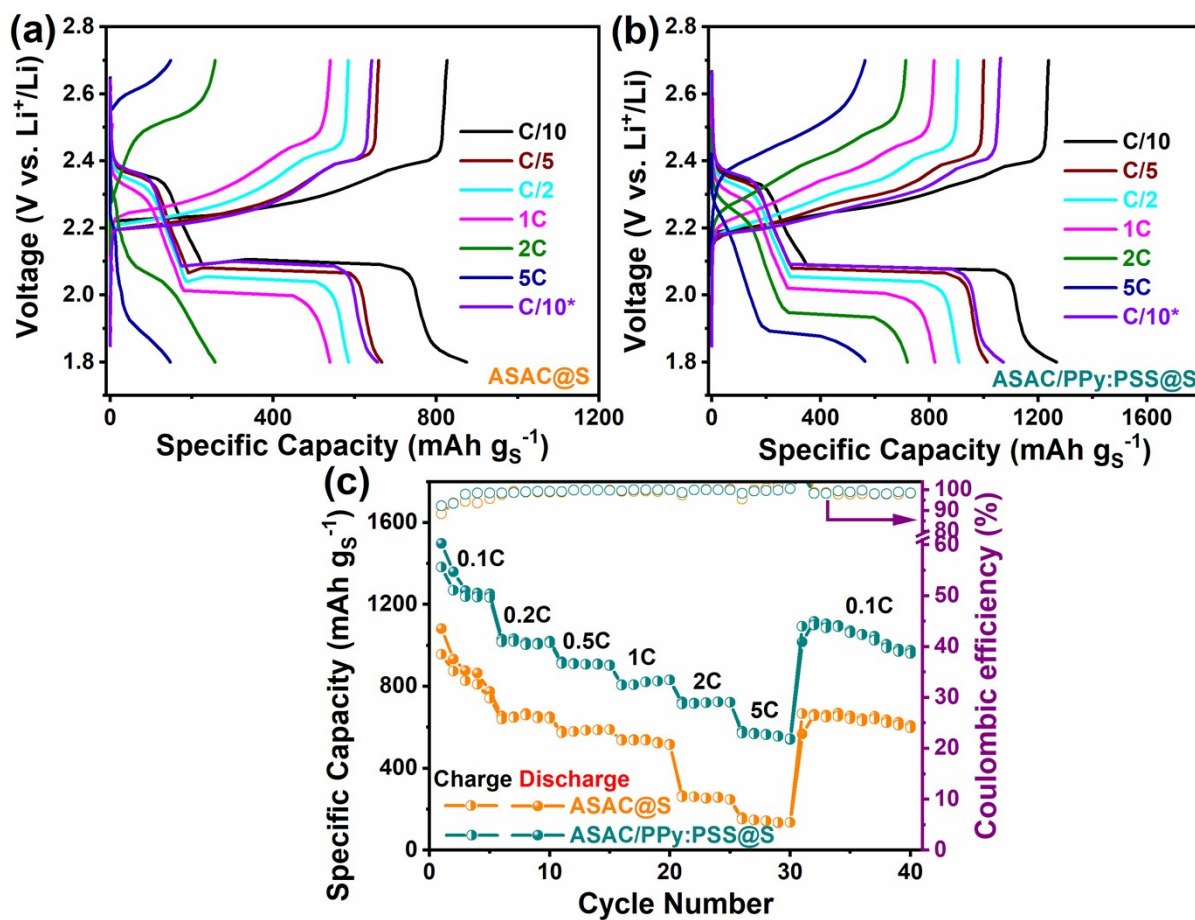


**Figure S16.** Rate capability data at different current rates for ASAC@S and ASAC/PPy:PSS@S composite electrodes with a sulfur loading of  $6 \text{ mg cm}^{-2}$ . Electrode sulfur loading:  $6.0 \text{ mg cm}^{-2}$ .

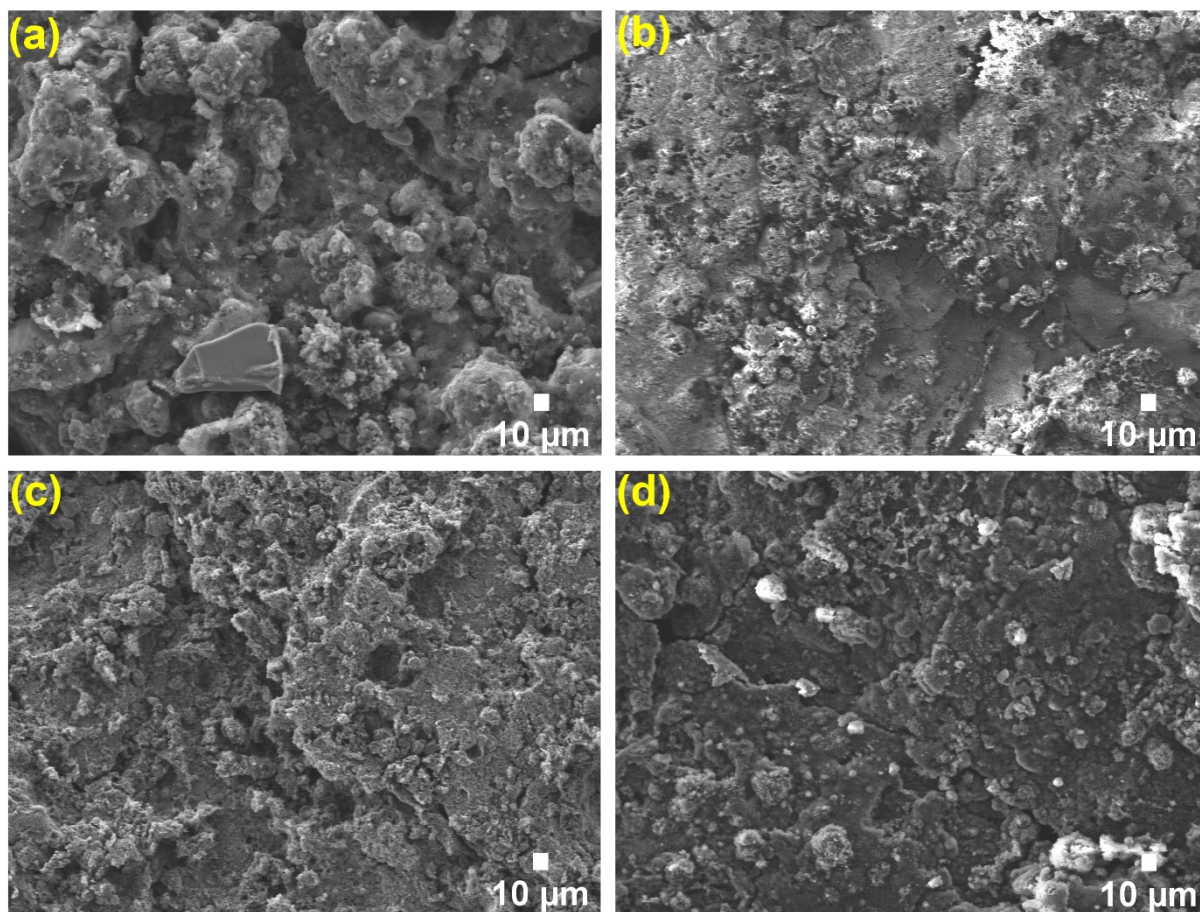


**Figure S17.** SEM images of electrodes: (a) ASAC@S uncycled, (b) ASAC@S cycled, (c) ASAC/PPy:PSS@S uncycled, and (d) ASAC/PPy:PSS@S cycled.